Biol. Cybern. 84, 103–115 (2001)

Biological Cybernetics
© Springer-Verlag 2001

An adaptive model of sensory integration in a dynamic environment applied to human stance control

Herman van der Kooij[1], **Ron Jacobs**[1,2], **Bart Koopman**[1], **Frans van der Helm**[1,3]

[1] Institute of Biomedical Technology, University of Twente, PO Box 217, 7500 AE Enschede, The Netherlands
[2] Intelligent Inference Systems Corporation, 107, West 333 Maude Avenue, Sunnyvale, CA 94086, USA
[3] Man-Machine Systems and Control Group, Delft University of Technology, Mekelweg 2, 2628 CD Delft, The Netherlands

Received: 12 November 1999 / Accepted in revised form: 30 June 2000

Abstract. An adaptive estimator model of human spatial orientation is presented. The adaptive model dynamically weights sensory error signals. More specific, the model weights the difference between expected and actual sensory signals as a function of environmental conditions. The model does not require any changes in model parameters. Differences with existing models of spatial orientation are that: (1) environmental conditions are not specified but estimated, (2) the sensor noise characteristics are the only parameters supplied by the model designer, (3) history-dependent effects and mental resources can be modelled, and (4) vestibular thresholds are not included in the model; instead vestibular-related threshold effects are predicted by the model. The model was applied to human stance control and evaluated with results of a visually induced sway experiment. From these experiments it is known that the amplitude of visually induced sway reaches a saturation level as the stimulus level increases. This saturation level is higher when the support base is sway referenced. For subjects experiencing vestibular loss, these saturation effects do not occur. Unknown sensory noise characteristics were found by matching model predictions with these experimental results. Using only five model parameters, far more than five data points were successfully predicted. Model predictions showed that both the saturation levels are vestibular related since removal of the vestibular organs in the model removed the saturation effects, as was also shown in the experiments. It seems that the nature of these vestibular-related threshold effects is not physical, since in the model no threshold is included. The model results suggest that vestibular-related thresholds are the result of the processing of noisy sensory and motor output signals. Model analysis suggests that, especially for slow and small movements, the environment postural orientation can not be estimated optimally, which causes sensory illusions. The model also confirms the experimental finding that postural orientation is history dependent and can be shaped by instruction or mental knowledge. In addition the model predicts that: (1) vestibular-loss patients cannot handle sensory conflicting situations and will fall down, (2) during sinusoidal support-base translations vestibular function is needed to prevent falling, (3) loss of somatosensory information from the feet results in larger postural sway for sinusoidal support-base translations, and (4) loss of vestibular function results in falling for large support-base rotations with the eyes closed. These predictions are in agreement with experimental results.

1 Introduction

To control posture, postural orientation must be known. Humans utilise multiple sources of sensory information to orient themselves in space. When the visual scene or support base is fixed, visual or proprioceptive information is sufficient to define postural orientation with respect to the gravitational axis and both can stabilise posture (e.g. Peterka and Benolken 1995; Ishida et al. 1997). However, support-base rotation or visual scene movement destabilise posture (e.g. Berthoz et al. 1979; Bolha et al. 1999).

Proprioceptive and visual clues alone are insufficient to distinguish ego-motion, visual scene and support-base motion from each other. In that case the vestibular system appears to be crucial in distinguishing ego-motion from environmental motion (see also Mergner et al. 1991, 1992, 1995). This is demonstrated by experiments in which for large movements of the visual scene (Peterka and Benolken 1995) or large platform rotations (Maurer and Mergner 1999), vestibular-loss patients – in contrast with normals – were not able to maintain balance. By the nature of the vestibular system, it is impossible to get an ideal estimate of orientation of the head in space, especially for low-frequency movements (Cohen et al. 1973; Mergner and Glasauer 1999). In most models of the

Correspondence to: H. Van der Kooij
(Tel.: +31-53-4894779; Fax: +31-53-4893471;
e-mail: h.vanderkooij@wb.utwente.nl)

vestibular system this non-ideal low-frequency behaviour is included as a physical threshold (e.g. Borah et al. 1988; Nashner et al. 1989; Hosman 1996). However, these thresholds are based on perceptual thresholds for ego-motion obtained from psychophysical studies (e.g. Clark and Stewart 1969). There is evidence that vestibular-related thresholds are of central origin and depend on other sensory clues (Mergner et al. 1995).

Among others (Borah et al. 1988; Gerdes and Happee 1994; Wolpert et al. 1995), we have described the complex process of human spatial orientation with the use of optimal estimation theory (Van der Kooij et al. 1999a). According to this view the control model has a kind of internal representation (IR) which includes 'knowledge' of the body and sensor dynamics, and the external environment. Using this representation the control model makes an estimate of spatial orientation using both the motor and sensory output signals. These sensory and motor signals are integrated so that a minimum variance estimate of postural orientation is obtained. Spatial orientation under various illusory sensations (Borah et al. 1988) and specific multivariate changes of postural sway due to altered visual or platform perturbation conditions (Van der Kooij et al. 1999b) can be predicted using optimal estimation theory. Optimal estimation theory, however, does not fully explain how humans integrate multisensory information. By using optimal estimation theory some 'knowledge' is required of the precision of the different sensory systems and of the external environment acting upon the body and the sensory system. This 'knowledge' is usually specified by power spectral density matrices of the sensor noise and of the disturbances acting on the body. These matrices are defined by the designer of the optimal estimator (Kalman filter) and are usually used as design variables. It is easy and tempting to use these power spectral matrices to match model predictions with experimental results. In models using a Kalman filter to model spatial orientation, the system and sensor noise statistics are used as 'tuning parameters' to mimic model with experimental results (Borah et al. 1988; Gerdes and Happes 1994; Wolpert et al. 1995). The statistical properties of external forces, support-base translations and rotation, and visual scene motion have to be specified in the human stance control model in order to obtain a minimum variance estimate of spatial orientation. The intriguing question of how humans solve the problem of distinguishing ego-motion from motion of the environment can not be understood within the concept of a non-adaptive observer like the (extended) Kalman filter; when using a Kalman filter the statistical properties of environmental motion are specified by the model designer.

Therefore, in this paper an adaptive estimator model of human spatial orientation is presented where, besides spatial orientation, 'knowledge' of the external environment is estimated from the sensory output signals instead of being specified by the designer. Only the sensor noise characteristics have to be specified by the model designer. We believe that the modified model is biologically more realistic. The model is used to investigate:

1. Whether it is possible to estimate postural orientation based on sensory information only and use this estimate to stabilise posture, without specifying environmental conditions as is done in existing models of spatial orientation.
2. Whether sensor noise properties can be found by matching model predictions with experimental results.
3. Whether the model produces vestibular-related thresholds without including physical thresholds.
4. Whether vestibular-related thresholds can be understood by the noisy properties of the sensory signals.
5. How sensory loss affects postural control and orientation under different environmental conditions.
6. Whether experience and cognitive resources can be modelled within this model, and how they influence postural orientation and control.

2 Methods

Optimal estimator models of spatial orientation are usually realised by including a Kalman filter (KF). The working of the KF is a combination of two processes. The first process uses the current estimate of spatial orientation and motor outflow to predict the next estimate of spatial orientation, by simulating the dynamics using an Internal Model (IM) of the body and environment. The second process uses an IM of the sensory dynamics to predict the sensory output corresponding to this predicted next estimate. The sensory error – the difference between actual and predicted sensory output – is weighted by the Kalman gain to drive the estimate of spatial orientation, resulting from the first process, to its true value. The elements of the Kalman gain are determined by the uncertainty in the predicted next estimate (caused for example by an imperfect IM or uncertainties of the environmental conditions) and the uncertainty in a sensory output signal. These uncertainties are specified by the designer of the KF as power spectral density matrices of the sensor noise and of the external environmental variables acting on the body. We modified our human stance control model (Van der Kooij et al. 1999a) by replacing the KF with and an adaptive KF. In the original model the statistical properties of mechanical disturbances, platform rotation and accelerations and visual scene motion, had to be specified by the model designer. In the modified model these statistical properties of the environment acting on the body are estimated by the adaptive KF simultaneously with the estimate of spatial orientation based on sensory and motor output signals only. Only the sensory noise levels have to be specified by the model designer and they are assumed to be stationary.

Besides replacing the extended with an adaptive KF, the following modifications to the model were made (Fig. 1):

1. Since, in this paper, we do not focus on inter-segmental co-ordination but on postural orientation in

space, the segment was reduced to an inverted pendulum model to save on computational requirements.
2. The model was linearised and converted to a discrete-time system with a sample time of 10 ms. The predictor, which compensates for neural time delays, is realised as a tapped delay line (Appendix A).
3. In the original model the visual scene was defined as either fixed in space or relative to the support base. The visual scene is now allowed to move. As a consequence, visual scene motion is defined in the IM of the environment as a state variable.
4. Vertical platform motion was excluded.
5. Tactile afferents other than the one sensing shear forces were not included in the model.

2.1 Adaptive sensory integration centre

To obtain an optimal estimate of spatial orientation, the environmental dynamics has to be included in the IM used by the KF (Van der Kooij et al. 1999a). After the above-mentioned modifications the IM is defined in discrete state-space format by:

$$\begin{bmatrix} \underline{x}_k^{\text{body}} \\ \underline{x}_k^{\text{env}} \end{bmatrix} = \begin{bmatrix} A^{\text{body}} & A^{\text{env2body}} \\ 0 & A^{\text{env}} \end{bmatrix} \begin{bmatrix} \underline{x}_{k-1}^{\text{body}} \\ \underline{x}_{k-1}^{\text{env}} \end{bmatrix} + \begin{bmatrix} B \\ 0 \end{bmatrix} u_{k-1} + \begin{bmatrix} 0 \\ G \end{bmatrix} \underline{w}_{k-1}^{\text{env}} \tag{1a}$$

$$\underline{y}_k = [H^{\text{body}} \; H^{\text{env}}] \begin{bmatrix} \underline{x}_k^{\text{body}} \\ \underline{x}_k^{\text{env}} \end{bmatrix} + Du_{k-1} + \underline{v}_k \tag{1b}$$

where:

$\underline{x}_k^{\text{body}}$ is the state vector of body and sensor dynamics, including the states of the sensor dynamics ($\underline{x}^{\text{sen}}$) and the orientation and velocity of the body with respect to the earth vertical axis (θ^{cq}, $\dot{\theta}^{\text{cq}}$). The sensor dynamics are obtained from the literature (Borah et al. 1988; Appendix B);

$\underline{x}_k^{\text{env}}$ is the state vector of the environment including the orientation of the support base with respect to the earth vertical (θ^{sb}), external forces acting on the body (F^{ext}), horizontal support base displacement, velocity and acceleration of the support base (s^{sb}, $\dot{s}^{\text{sb}}$, $\ddot{s}^{\text{sb}}$) and the position of the visual scene (s^{vis});

u_{k-1} is the control to stabilise the body generated by a proportional-derivative (PD) controller;

$\underline{w}_{k-1}^{\text{env}}$ are the random forcing functions of the environmental variables;

$\underline{y}_k$ is the sensory output;

$\underline{v}_k$ is the sensory output noise;

A^{body} is the representation of the body and sensor dynamics;

A^{env2body} is the representation of the effect of the environment on body and sensor dynamics;

A^{env} is the representation of environmental dynamics;

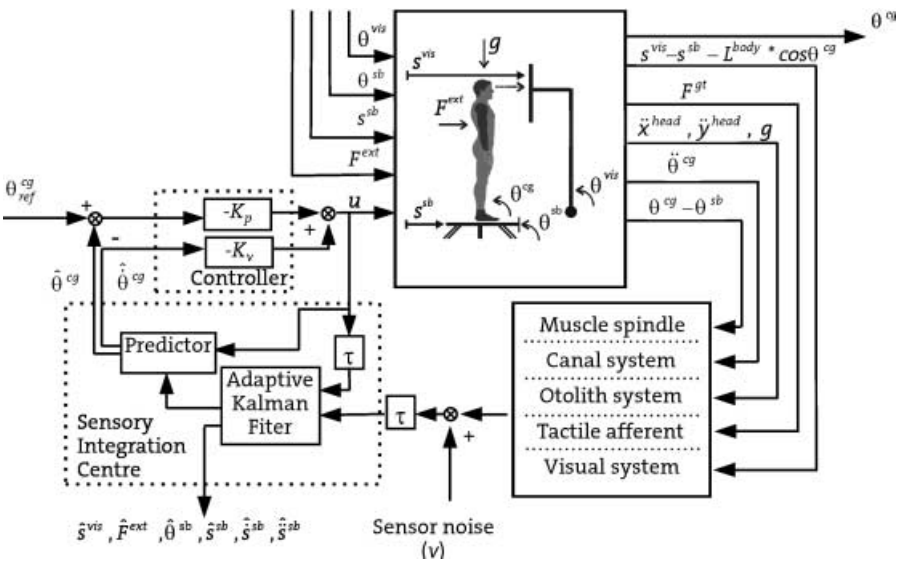

Fig. 1. Schematic view of the modified human stance control model. Standing person is modelled as an inverted pendulum exposed to environmental variables. The person stands on a support base, which can translate (s^{sb}) and rotate (θ^{sb}). External forces acting on the body are support-base accelerations, external forces (F^{ext}), and gravity (g). The modelled person looks at a visual scene at distance s^{vis}. The visual scene can rotate around an axis (θ^{vis}). Different sensor systems are modelled. Input to the muscle spindle is ankle joint angle. Input to the canal systems is angular acceleration of the head. Inputs to the otolith system are gravitational and linear accelerations of the head. Input to the visual system is the distance between the head and the visual scene. Input to the tactile afferents is shear force at the sole. Based on delayed sensory output signals and synchronised control inputs, an adaptive Kalman filter estimates postural orientation and environmental conditions for times $t - \tau$. A predictor compensates for the neural time delays ($\tau = 100$ ms). The controller to stabilise posture with respect to the desired orientation uses the resulting estimate of spatial orientation

B	is the control input distribution matrix;
G	is the noise output matrix;
H^{body}	is the mapping of the body states onto the sensory output vector;
H^{env}	is the mapping of the environmental states onto the output vector;
D	is the mapping of the control inputs onto the sensory output vector.

In compact form (1) is given by:

$$\underline{x}_k = A\underline{x}_{k-1} + Bu_{k-1} + \underline{w}_{k-1} \tag{2a}$$

$$\underline{y}_k = H\underline{x}_k + Du_{k-1} + \underline{v}_k \tag{2b}$$

The random vectors $\underline{w}_{k-1}$ and $\underline{v}_k$ are treated as independent, non stationary, Gaussian, white noise sequences with the properties

$$E[\underline{w}_i] = 0,\ E[\underline{w}_i\underline{w}_j] = Q_i\delta_{ij} \tag{3a}$$

$$E[\underline{v}_i] = 0,\ E[\underline{v}_i\underline{v}_j] = R_i\delta_{ij} \tag{3b}$$

where Q_i and R_i are true moments about the mean of the state and sensory output noise sequences, respectively. Since changes in the external world are not known a priori, these possible changes are included in the IM as random walks; i.e. a differential equation with stochastic inputs ($\underline{w}$) (Van der Kooij et al. 1999a; Appendix C). In our model, the strength of the state noise, $\underline{w}$, is related to the first derivatives of support-base rotations, external disturbances, horizontal support-base accelerations and visual scene motion (Appendix C). So, in our model the state noise is directly related to the physics of the external world. The state noise only exists in the IM to model the external world, but is not put into the model of the standing person (in Fig. 1, $\underline{w}$ is not put into the model). Since in this paper only finite motions of the environment are considered, the assumption that $\underline{w}$ is zero mean distributed (3a) is not restricting.

An optimal estimate for the system defined by (2) is obtained with the standard KF: (Gelb, 1974)
state propagation

$$\begin{aligned}\bar{\underline{x}}_k &= A\hat{\underline{x}}_{k-1} + Bu_{k-1}\\ \bar{P}_k &= A\hat{P}_{k-1}A^{\mathrm{T}} + Q_{k-1}\end{aligned} \tag{4a}$$

observation residual

$$\underline{z}_k = \underline{y}_k - H\bar{\underline{x}}_k \tag{4b}$$

Kalman gain

$$K_k = \bar{P}_k H^{\mathrm{T}}[H\bar{P}_k H^{\mathrm{T}} + R_k]^{-1} \tag{4c}$$

state estimation

$$\begin{aligned}\hat{\underline{x}}_k &= \bar{\underline{x}}_k + K_k\underline{z}_k\\ \hat{P}_k &= \bar{P}_k - K_k H\bar{P}_k\end{aligned} \tag{4d}$$

where $\bar{\underline{x}}_k$ and $\bar{P}_k$ are the propagated state and error covariance conditioned on observations prior to time t_k. $\hat{\underline{x}}_k$ and $\hat{P}_k$ are the estimated values after the new sensory output vector $\underline{y}_k$ has been processed. When the statistics of state noise and sensor noise are known as a function of time, the KF supplies an optimal estimate. However, in many applications these statistics are not known a priori. In most applications these statistics are assumed constant and chosen a priori, based on experimental data or design criteria.

An optimal filter for state estimation under unknown noise statistics does not exist (Myers and Taply 1976). Many suboptimal schemes have been derived. All methods can be classified into two approaches: (1) the direct approach identifying the KF gain from the data directly (e.g. Juan et al. 1993), and (2) the indirect approach estimating the noise statistics first and then using them to compute the Kalman filter gain (4). We followed the second approach. We modified the method of Myers and Taply (1976), to sequentially estimate the state noise statistics. We assumed that the sensor noise statistics (R) are constant and known. Myers and Taply derived an unbiased estimator for Q given by (Appendix D):

$$\hat{Q} = \frac{1}{N-1}\sum_{j=1}^{N}\left\{(\underline{q}_j - \hat{\underline{q}})(\underline{q}_j - \hat{q})^{\mathrm{T}} - \left(\frac{N-1}{N}\right)\left[A\hat{P}_{j-1}A^{\mathrm{T}} - \hat{P}_j\right]\right\} \tag{5a}$$

$$\hat{\underline{q}} = \frac{1}{N}\sum_{j=1}^{N}\underline{q}_j \tag{5b}$$

$$\underline{q}_j \equiv \hat{\underline{x}}_j - A\hat{\underline{x}}_{j-1} - Bu_{k-1} \tag{5c}$$

After the state estimation (4d), Q_k is estimated based upon the last N noise samples $\underline{q}_j$ ($j = k - N + 1, \ldots, k$) at time t_k. The diagonal elements of $\hat{Q}$ are always reset to the absolute values of their estimates. For first N time-steps of the simulation, Q is set to the initial value $Q_0 = GQ_0^{\text{env}}$ and $\hat{Q}$ is estimated for $k > N$.

2.2 Evaluation of the adaptive sensory integration model

First, the minimal set of sensory systems was determined for which it was possible to obtain a stable estimate of postural orientation without specifying environment conditions. External disturbances (F^{ext}) and support-base displacements (s^{sb}) were applied to the model. Sensory output signals were assumed to be ideal, i.e. not distorted with noise ($R \sim O$). Next, the effect of imperfect sensory signals was investigated by adding white noise to the sensory output signals. Model responses to sinusoidal[1] movements of the visual scene were compared with experimental results of visually induced

[1] It is better to use stochastic inputs instead of sinusoidal inputs to obtain the frequency response function of a closed-loop system. However, in order to compare model responses with reported experimental results, sinusoidal inputs were applied to the model

sway. Finally, model responses to sinusoidal support-base rotations were calculated and qualitatively compared with experimental findings. For all simulations the mass of the pendulum was 80 kg, the length 1.8 m, the height of center of mass (CoM) 1.1 m, and the moment of inertia around CoM 24.8 kg m^2. For all simulations the controller was implemented as a PD controller with $K_p = 1815$ and $K_v = 560$. The number of samples used to estimate Q was $N = 16$. The initial value of Q was $Q_0 = GO_0^{\text{env}}$ with $Q_0^{\text{env}} = I^* \, 1\text{e}-9$, where I is a 4×4 unity matrix. To initialise the filter for the first 14 seconds only sensory noise was put into the model.

2.2.1 Minimal set of sensory systems. At first, the modelled sensory systems were assumed to be ideal; sensory output signals were not distorted with noise ($R \sim 0$). Disturbances applied to the model were either a combination of sinusoidal external disturbances (F^{ext}) applied at a height of 1 m, and support displacements (s^{sb}) or external disturbances only. The frequency of F^{ext} was 1 Hz and the amplitude 10 N. The frequency of s^{sb} was 0.5 Hz and its amplitude 10 cm. The ability to maintain standing was examined for different scenarios: (1) non-rotating support base and fixed visual scene, (2) sway referencing the support base, keeping the ankle joint constant, (3) sway referencing the visual scene, keeping visual input constant, and (4) simultaneously sway referencing the support base and visual scene. Sway referencing the support base or visual scene is a technique to position the support base or visual scene in such a way that the orientation and/or distance of the support base or visual scene remains constant relative to the body, thereby eliminating proprioceptive and visual clues about postural orientation with respect to the earth vertical.

Sway referencing the visual scene and support base was initiated at the start of applied perturbations. To obtain minimal sets of sensory systems for the four different scenarios, sensory loss was simulated by removing the corresponding sensory system from the model. Normalised peak-to-peak amplitudes of centre of gravity (CG) sway angle ($\theta_{\text{cg}}(t)$) are used to quantify the effect of sensory loss for the four different scenarios. Peak-to-peak amplitudes of postural sway were normalised to the condition for which the visual scene was fixed, the support base was not rotating, and no sensory loss was modelled.

2.2.2 Model responses to sinusoidal visual scene displacements. The effect of imperfect sensory signals was studied by adding white noise to the sensory output signals. Sensory noise was applied to the model for the: (1) muscle spindle, (2) canals, (3) otoliths, (4) visual system, and (5) tactile afferents (Fig. 1). The strength of the noise for the five different sensory systems was determined by trying to mimic the experimental results of visually induced sway (Peterka and Benolken 1995). Appropriate noise levels were found by trial and error. Different sinusoidal visual scene displacements were applied to the model. The following specifications of the simulations are adapted in agreement with the experiments of Peterka and Benolken (1995). The visual scene rotated around an axis that was co-linear with the ankle joint axis and was located about 10 cm above the ankle (in Fig. 1, $s^{\text{vis}} = 0.65 - (1.80 - 0.1) \cdot \sin(\theta^{\text{vis}} - \pi/2)$). The visual scene was located about 65 cm from the eyes. The model was evaluated for fixed and for sway referenced support base conditions. Removing the vestibular organ from the model simulated the performance of vestibular-loss patients. The visual scene was sinusoidally rotated at two different frequencies (0.1 Hz and 0.2 Hz) and at six different amplitudes (0.2°, 0.5°, 1°, 2°, 5° and 10°). All combinations were applied for 60 s. All trials were repeated 30 times with the same initial settings in order to average the effect of sensor noise. Sway referencing was initiated at the start of the sinusoidal visual scene motion. The CG sway angle was used to evaluate the model response. Fourier analyses of the CG angle and the visual scene angle time series were used to calculate the amplitude of the CG sway relative to visual scene motion. The discrete-time Fourier transform of sampled CG sway angle and the visual scene angle time series evaluated at frequency f are defined as:

$$\theta^{\text{cg}}(f) = F[\theta^{\text{cg}}(i)] \tag{6a}$$

$$\theta^{\text{v}}(f) = F[\theta^{\text{v}}(i)] \tag{6b}$$

where $\theta^{\text{cg}}(i)$ is the sampled CG sway angle and $\theta^{\text{v}}(i)$ is the sampled visual scene angle time series from the simulations.

The frequency-response function between the visual stimulus and CG sway is defined as:

$$H_{\text{v2cg}}(f) = \frac{\theta^{\text{cg}} f}{\theta^{\text{v}}(f)} \tag{7}$$

In general it is better to use the cross-spectral density to calculate the frequency-response function. However, since the data of Peterka and Benolken (1995) is used, their approach is adopted and the quotient of the Fourier transform of input and output signals is used to calculate the frequency-response function.

The first cycle of CG angle and visual scene angle time series were excluded from the Fourier analysis. Fourier analysis was performed over a range of frequencies to test whether the model showed a clear response to the visual stimuli. Amplitudes of the CG sway and of the frequency-response function were calculated at the frequency of the visual stimulus.

2.2.3 Model responses to sinusoidal support-base rotation. Different sinusoidal support-base rotations were applied to the model, the same as those applied in the experiments Bolha et al. (1999). The noise levels found earlier were applied to the model. The model was evaluated for eyes open and eyes closed. Removing the visual system from the model simulated the eyes closed condition. The support base was sinusoidally rotated at two different amplitudes (1° and 4°) and at six different frequencies (0.025 Hz, 0.05 Hz, 0.1 Hz, 0.2 Hz, 0.4 Hz, and 0.8 Hz). After initialising the filter, all combinations

were applied for 60 seconds. All trials were repeated 30 times with the same initial settings in order to average the effect of sensor noise. The frequency-response function between the support-base rotation and the CG sway ($H_{sb2cg}(f)$) was obtained in the same way as $H_{v2cg}(f)$ (7).

3 Results

3.1 Minimal set of sensory systems

The model is able to resist external forces in the case of ideal sensory output signals from muscle spindles, the vestibular organ, the visual system, and tactile afferents sensing shear forces from the sole (Table 1, A). Even for sensory conflict conditions, like sway referencing the support base or the visual scene, the model predicts a stable posture. Loss of somatosensory or visual information hardly affects posture, even when both the visual scene and the support base are sway referenced (Table 1, B, D and E). Without vestibular function the model predicts stable standing if the visual scene and support base are fixed (Table 1, C1). However, in case of sensory conflicts the vestibular organ seems to be crucial. Without a vestibular system, the model is not able to obtain a stable estimate of posture, and falls are predicted for those cases where sensory conflicts occur in combination with small external disturbances (Table 1, C2–C4). Surprisingly, the model predicts a decrease in CG sway when proprioception is excluded. Although the relative differences are considerable, the absolute differences are very small (maximal 0.05°). The differences are difficult to interpret since only one specific stimulus was applied to the model.

Table 1. Effect of sensory loss in the presence of external disturbances. Four different scenarios are considered: (1) fixed support base and visual scene, (2) sway referencing the support base, (3) sway referencing the visual scene, and (4) sway referencing the support base and visual scene. The effect of sensory loss was modelled by removing different sensory systems. Shown are the amplitudes of the CG sway angles, normalized to condition (A1): fixed visual scene, non-rotating support base and no sensory loss. In some conditions the model predicted instability (denoted by *crosses*). *Stars* indicate excessive initial responses at the onset of the disturbance

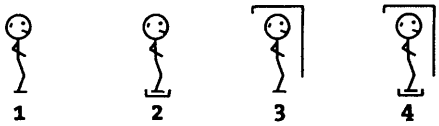

Sensory loss	1	2	3	4
A: No Loss	1	0.7	1	0.7
B: Muscle spindle	0.8	0.9	1	1
C: vestibular	1*	X*	X	X
D: vision	1	0.7	-	-
E: Tactile	0.8	1*	1	1*

These results are in agreement with the experimental results of the sensory organization test (SOT) for normals and vestibular-loss patients (Black et al. 1988). Normals were able to maintain standing during the SOT, even when the support base or the visual scene was sway referenced. Vestibular-loss patients were able to maintain standing when sensory conflicts were absent. However, in the case of sway referencing the support base or the visual scene, the majority were unstable for these sensory conflict situations.

When all sensory systems are included, the model is able to resist a combination of external forces and support base displacements (Table 2, A). The effect of somatosensory loss is different compared to the situation without support base displacements (Table 1). Removing the muscle spindles or tactile afferents from the model results in an increase in CG sway by a factor of four (Table 2, B and E). For additional sinusoidal support-base displacements, the effect of vestibular loss is even worse compared to the case of external forces only. After removal of the vestibular system the model is not able to maintain standing even when the support base is not rotating and the visual scene is fixed (Table 2, C).

Not much is known about the contribution of skin afferents to postural control. However, after anaesthesia of both feet and ankles, subjects altered their postural responses to sudden support-base displacements resulting in excessive body sway (Horak et al. 1990). This experimental finding is in agreement with the predicted increase in CG sway during platform translations due to loss of tactile afferents (Table 2, E) or loss of muscle spindles (Table 2, B). However, also in this case we should be careful since only one specific stimulus was applied to the model.

The inability of the model to stabilise posture without vestibular function – but with reliable visual and muscle spindle input (Table 2, C1) – is at first glance surprising. Vestibular-loss patients are able to maintain standing when exposed to sudden support-base displacements even with eyes closed (Runge et al. 1998). The difference with the model simulations is that these experiments studied the effect of short support-base translations of a few centimetres. However, vestibular-loss patients will

Table 2. Same as Table 1, but showing the effect of sensory loss in the presence of simultaneously external disturbances and support-base translations

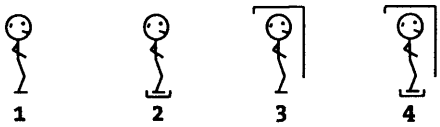

Sensory loss	1	2	3	4
A: No Loss	1	1	1	1
B: Muscle spindle	4	4	4	4
C: vestibular	X	X	X	X
D: vision	1	1	-	-
E: Tactile	4	4*	4*	4

fall when exposed to continuous sinusoidal translations of the support base even with eyes open (Buchanan and Horak 1998).

3.2 Model responses to sinusoidal visual scene displacements

The variance of signal noise for muscle spindles is: $V_{\text{spin}} = 1.1\text{e} - 6$; for sole afferents: $V_{\text{sole}} = 33$; for semicircular canals: $V_{\text{sem}} = 0.21$; for otoliths: $V_{\text{oto}} = 65$; and for vision: $V_{\text{vis}} = 1.2\text{e} - 5$. For these noise intensities, the model predictions match the experiment results (Fig. 2). The amplitude of model-predicted visually induced sway in normals depends upon stimulus frequency, stimulus amplitude, and support-base condition (Fig. 2). The amplitude of CG sway for sway referenced conditions is larger than for fixed support-base conditions, for any stimulus frequency and amplitude. The amplitude of CG sway increases with stimulus amplitude until a saturation level is reached. For sway referenced conditions the saturation level is four times higher than for fixed support-base conditions. The saturation level decreases with increasing stimulus frequency. The instant at which saturation occurs also depends upon stimulus frequency and support-base condition. For sway referenced conditions and for faster stimulus frequencies the CG sway saturates at larger stimulus amplitudes.

In fixed support-base conditions the gain for normal subjects is always less than unity (Fig. 3). For sway referenced support-base conditions, the gain is larger than unity for small stimulus amplitudes. The gain decreases in proportion with the logarithm of stimulus amplitude until the saturation effect occurs. Again, model simulations are similar to the experimental results. In Fig. 3 the non-linear input-output behaviour is clearly seen; for linear systems, the gain would not be dependent on the amplitude of the input stimulus.

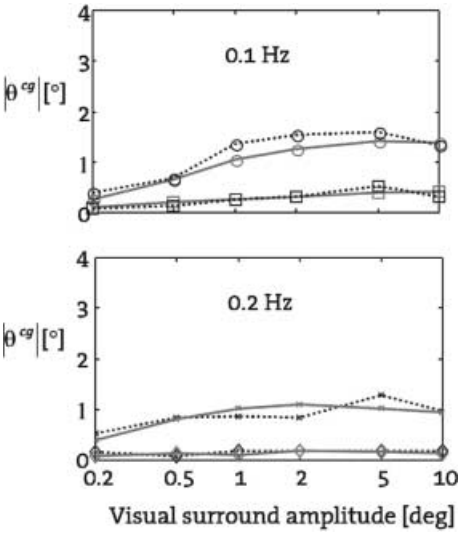

Fig. 2. Mean centre of gravity (CG) sway amplitude induced by visual scene motion as a function of stimulus amplitude. Model prediction (*solid lines*) and experimental results (*dotted*; Peterka and Benolken 1995) in normal subjects. *Top*: stimulus frequency 0.1 Hz; *bottom*: stimulus frequency 0.2 Hz. Support base was fixed (*boxes* and *diamonds*) or sway referenced (*circles* and *crosses*)

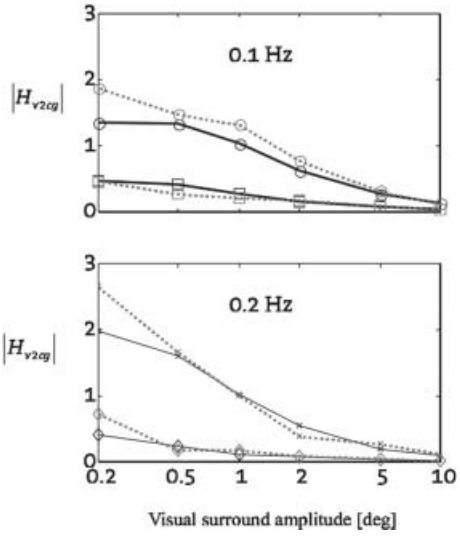

Fig. 3. Gain of mean CG sway amplitude induced by visual scene motion as a function of stimulus amplitude. Model prediction (*solid lines*) and experimental results (*dotted*; Peterka and Benolken 1995) in normal subjects. *Top*: stimulus frequency 0.1 Hz; *bottom*: stimulus frequency 0.2 Hz. The support base was fixed (*boxes* and *diamonds*) or sway referenced (*circles* and *crosses*)

Sensory errors arise due to sensory output noise, external forces, and motion of the environment. It can be clearly seen that for the smallest amplitude of visual scene motion the sensory errors are dominated by sensory output noise (Fig. 4, left and middle). For the largest amplitude of visual scene motion, the visual scene motion can be clearly seen in the sensory errors (Fig. 4, right). From Fig. 4 it can also be understood why the sensory output noises of the different systems differ dramatically. Due to different sensor dynamics (Appendix B), the sensitivity of the sensory organs differs as reflected in the sensory errors (Fig. 4, right). The sensory output noises that were found are in proportion to the changes in sensory output signal due to ego-motion or motion of the environment.

Stimulation results of CG sway in vestibular-loss patients compared to the CG sway in normals for fixed support-base conditions are shown in Fig. 5. For low stimulus amplitudes the model predictions for normals and vestibular-loss patients are similar. However, at larger stimulus amplitudes, the saturation effect does not occur for vestibular-loss patients. The model results of vestibular-loss patients diverge from normals at higher stimulus amplitudes. The amplitude where the results diverge depends on stimulus frequency: for faster stimuli the results diverge at lower stimulus amplitudes. For large stimulus amplitudes the model predicts that the falling of patients is caused mainly by excessive transient response at the onset of the stimulus (results not shown). These results for vestibular-loss patients agree well with experimental results (Peterka and Benolken 1995). Whereas in the experiment vestibular-loss patients were

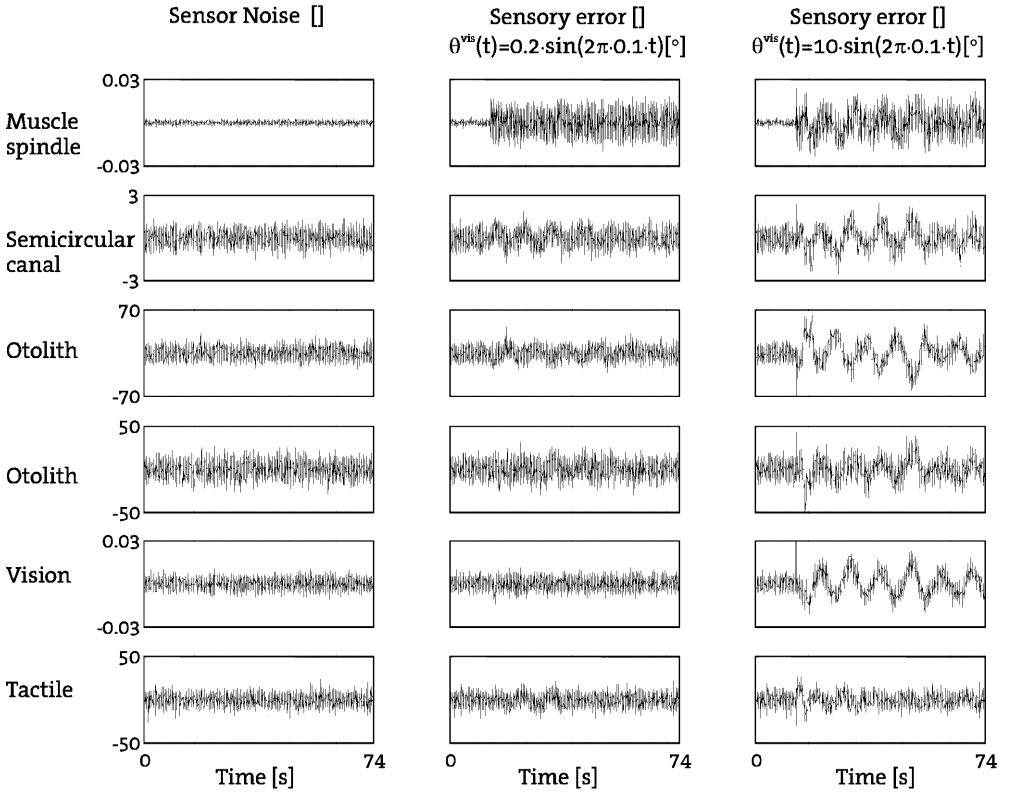

Fig. 4. Noise properties of sensor-related signals. *Left*: typical example of sensory output noise v_k in the different sensory systems. *Middle*: typical example of sensory errors (4b) in the case of visually induced sway with a small stimulus amplitude and a sway referenced support base. *Light*: typical example of sensory errors in the case of visually induced sway with a large stimulus amplitude and a sway referenced support base. Note that the stimuli were applied after 14 s

able to maintain standing for small stimuli amplitudes while the support base was sway referenced, the model was not able to estimate a stable posture for these conditions.

3.3 Model responses to sinusoidal support-base rotation

The model-predicted CG sway for sinusoidal support-base rotations is given by the gain of the frequency response function $H_{\mathrm{sb2cg}}(f)$ (Fig. 6). The predicted gain shows a peak at 0.1 Hz. For slower stimulus frequencies the gain is lower. For frequencies higher than 0.1 Hz, the gain decreases and for normals reduces almost to zero for a stimulus frequency of 0.8 Hz. Gain characteristics also depended upon stimulus amplitude and visual condition. The gain decreases for larger stimuli amplitudes at any stimulus frequency and at any visual condition. For eyes closed, the gain at any stimulus frequency and amplitude is higher than for eyes open. The simulation results of vestibular-loss patients show larger gain characteristics when compared to normals. For low stimulus frequencies vestibular-loss patients cannot suppress muscle spindle input, even when the subjects had their eyes open (Fig. 6). For large support-base rotations falling will result. However, the model predicts that they are able to suppress muscle spindle input at larger stimuli frequencies, thereby preventing themselves from falling.

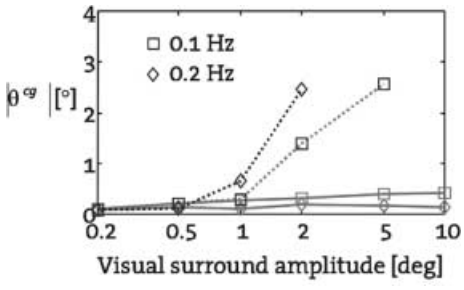

Fig. 5. Gain of mean CG sway amplitude induced by visual scene motion as a function of stimulus amplitude. Model prediction of normal subjects (*solid lines*) and vestibular loss patients (*dotted lines*). *Boxes*: stimulus frequency 0.1 Hz; *diamonds*: stimulus frequency 0.2 Hz. The support base was fixed

These results are in agreement with the experimental study of Bolha et al. (1999). In this study the same stimuli were used for which Bolha et al. found a 'dip' in postural control performance at 0.1 Hz. This 'dip' was partially compensated by the visual system. The model predicts falling of vestibular-loss patients for large slow platform rotations even when the subjects had their eyes open. This is in agreement with experimental findings where vestibular-loss patients indeed fell during support base rotations of 8° with a dominant frequency of 0.2 Hz (Maurer and Mergner 1999).

The effect of experience or knowledge of the experimental set-up was studied by resetting the initial value of $Q_0 = GQ_0^{\mathrm{env}}$. The element of Q_0^{env} corresponding to support rotations was changed from 1e−19 to 1. This can be interpreted as the expectation that the support base will rotate, which results in a smaller response to support-base rotations (Fig. 7). The effect of the initial setting is larger for eyes open and for lower stimuli frequencies.

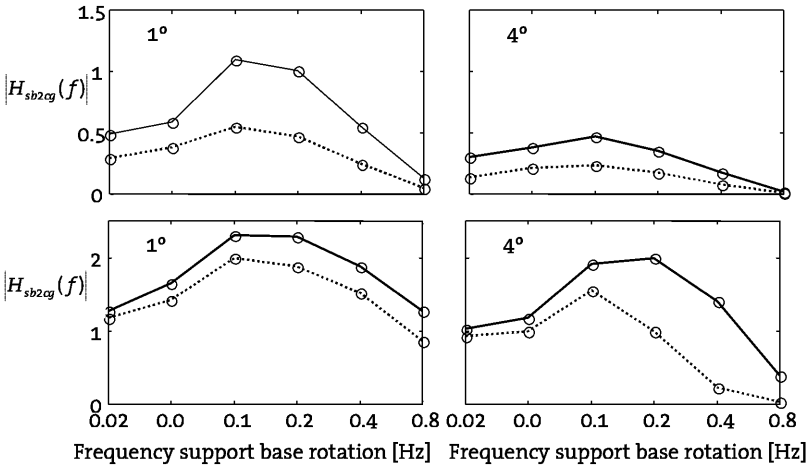

Fig. 6. Model-predicted gain of mean CG sway amplitude induced by rotational motion of the support base as a function of stimulus frequency. *Left*: stimulus amplitude 1°; *right*: stimulus amplitude 4°. *Top*: normal subjects; *bottom*: vestibular-loss patients. Eyes were open (*dotted lines*) or closed (*solid lines*)

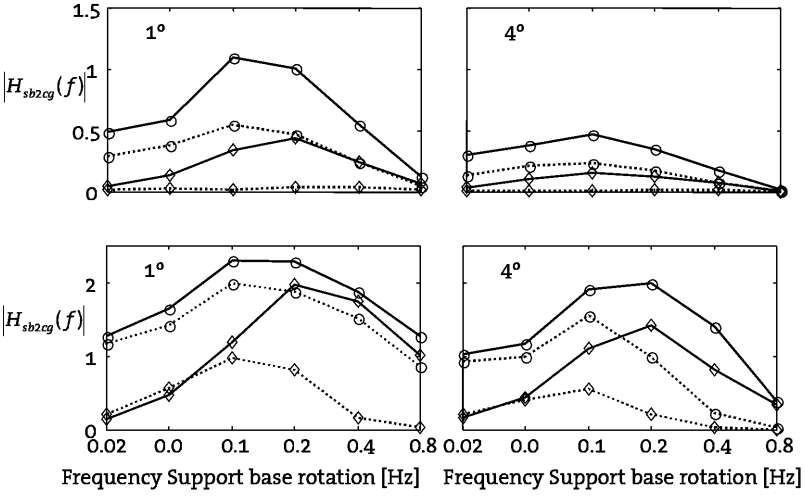

Fig. 7. Model-predicted gain of mean CG sway amplitude induced by rotational motion of the support base as a function of stimulus frequency. The effect of experience or 'knowledge' of the experimental set-up was studied by resetting the initial value of $Q_0 = GQ_0^{\mathrm{env}}$. The element of Q_0^{env} corresponding to support rotations was changed from 1e−19 (*circles*) to 1 (*diamonds*). This can be interpreted as anticipating a support-base rotation. *Left:* stimulus amplitude 1°; *right*: stimulus amplitude 4°; *Top*: normal subjects; *bottom*: vestibular-loss patients. Eyes were open (*dotted lines*) or closed (*solid lines*)

4 Discussion

Previous work (Van der Kooij et al. 1999a) demonstrated that to obtain a minimum variance estimate of spatial orientation, humans should have:

1. An internal representation of the dynamics of the body, the sensory systems, and the environment.
2. Knowledge of the precision of the different sensory systems.
3. Knowledge of the amount of changes in visual scene motion, motion of the support base, and external forces acting on the body.

When the dynamics are linear this minimum variance estimate is an optimal estimate. Spatial orientation can be estimated optimally only if these three conditions are satisfied. In our previous work, we assumed that these three conditions were fulfilled. It is reasonable to assume that due to a learning process humans have a knowledge of the dynamic properties of their own body and their environment, and of the reliability of their sensory organs. However, the assumption that humans have a (correct) knowledge of the amount of changes in the environmental conditions is non-trivial. This is demonstrated by common illusionary sensations where ego-motion and motion of the environment are misinterpreted. A well-known illusionary ego-motion perception is the illusion that the train you are in is moving, whereas actually the train on the other track is moving.

In the modified model we do not have to quantify the changes in environmental conditions, as we have to in the optimal model. These properties are now directly estimated from sensory output signals, resulting in a dynamical weighting of sensory error signals depending on environmental conditions. The modified model was applied to human stance control. With only five model parameters specifying the precision of the sensory systems, experimental results of a visually induced sway experiment (Peterka and Benolken 1995) could be reproduced. The model predicted far more than five data points, suggesting a strong predictive capacity. Moreover, the model predictions for slow platform rotations qualitatively resembled experimental results presented by Bolha et al. (1999). Model predictions show that:

1. Vestibular function is necessary to solve sensory conflicts.
2. Vestibular function is not crucial when sensory conflicts are absent.
3. Tactile afferents in the feet play an important role when the support base is translating.

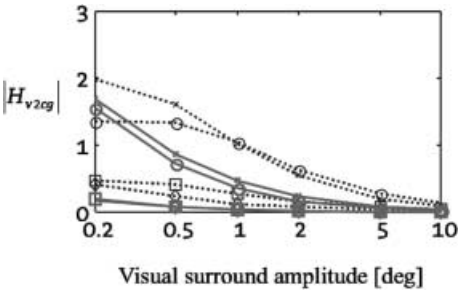

Fig. 8. Gain of mean CG sway amplitude induced by visual scene motion as a function of stimulus amplitude. Model prediction of the optimal (*solid lines*) and the adaptive (*dotted lines*) model. *Boxes*: the support base was fixed, stimulus frequency 0.1 Hz; *diamonds*: the support base was fixed, stimulus frequency 0.2 Hz; *circles*: the support base was sway referenced, stimulus frequency 0.1 Hz; *crosses*: the support base was sway referenced, stimulus frequency 0.2 Hz

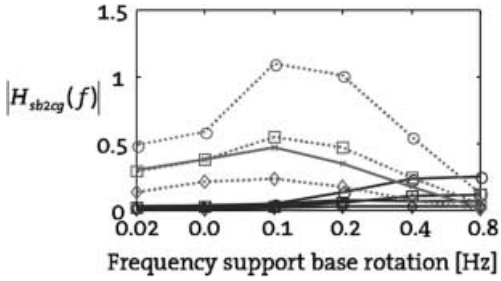

Fig. 9. Gain of mean CG sway amplitude induced by rotational motion of the support base as a function of stimulus frequency. Model prediction of the optimal (*solid lines*) and the adaptive (*dotted lines*) model. *Boxes*: eyes open, stimulus amplitude 1°; *diamonds*: eyes open, stimulus amplitude 4°; *circles*: eyes closed, stimulus amplitude 1°; *crosses*: eyes closed, stimulus amplitude 4°

4. Responses to motion of the visual scene and to support-base rotation are highly non-linear. The gain depends on stimulus amplitude and frequency, and on support-base condition (fixed or sway referenced).

All these model predictions are consistent with experimental results. The presented adaptive model of sensory integration is more realistic than the previously developed model (Van der Kooij et al. 1999a) and other models of spatial orientation. It requires less assumptions and model input parameters. Moreover, model predictions and experimental results of visually induced sway suggest that postural orientation can not always be estimated optimally. Intuitively, to obtain an optimal estimate of postural orientation when standing on a fixed support visual scene motion should be ignored, since visual clues in this particular case cause an illusionary perception of ego-motion. Model simulations of visually induced sway with the optimal model confirm this intuitive finding. In contrast to the adaptive model, the optimal model predicts almost no response to visual scene motion, especially for larger stimulus amplitudes (Fig. 8).

Moreover, model simulations of support base rotations (Fig. 9) also show that predictions of the adaptive model (this paper) and the previous model (Van der Kooij et al. (1999a) do not coincide. The differences are more pronounced for small and slow motions.

The fact that postural responses are shaped by a person's experience, intent, knowledge, and instruction (Jacobs et al. 1997) is further evidence for the hypothesis that postural orientation and control is not (always) an optimal process. In the model this dependency is demonstrated by the setting of the initial value Q_0. In this study, the initial value was reset for each simulation. But in general Q_0 depends on prior experience, instruction or knowledge, for example of an experimental protocol.

The vestibular organ is needed to distinguish ego-motion from the motion of the environment. Especially for slow and small movements, humans are not able to distinct ego-motion from environmental motion as demonstrated by experiments and model predictions. In most models of spatial orientation this non-ideal or non-optimal behaviour is included as a physical threshold that is related to vestibular output signals. The existence of a perceptual threshold is proven (e.g. Hosman 1996). However, there is no evidence for a physical threshold. Interestingly, the modified model predicted a vestibular related threshold: the saturation of visually induced CG sway for sway reference condition is related to a vestibular threshold (Peterka and Benolken 1995).

In addition, the model gives insight into the origin of vestibular-related thresholds. Noisy sensory error signals – the difference between expected and actual sensory output signals – are used to obtain an estimate of spatial orientation of posture and environment. Sensor noise and changes in the external world (visual scene, support base, forces) cause sensory errors. During slow and small motion of the environment, the error signals related to the vestibular system are dominated by noise in the vestibular output signal (e.g. Fig. 4). Therefore, these error signals are almost useless when updating the estimate of spatial orientation and the amount of movement of the environment, causing sensory illusions. This however, does not imply, the existence of high biological noise levels in vestibular output signals. Prediction of high noise levels for a particular sensory output signal should be interpreted so that the signal of the corresponding sensory system is modelled unreliably.

In the present model it is hypothesised that humans have a kind of internal representation of the dynamics of the body, the sensors and the external world, and have knowledge of the precision of different sensory systems. There is much debate about the existence and location of internal presentations in the brain that mimic the behaviour of the sensorimotor system and the external world. Only indirect evidence of the existence of these internal representations is available (e.g. Kawato and Wolpert 1998; Wolpert et al. 1998; Angelaki et al. 1999; Merfeld et al. 1999; Imamizu et al. 2000). An interesting question is to what level of detail these internal representations should correspond with reality. Should these internal representations capture only the kinematics, or should they capture both the kinematics and the dynamics? In the present paper, the internal model was an exact copy of the actual dynamics of the body, the sensors, and the external world. In the future we will study the effect of imperfect internal models by adding additional state noise or simplifying the internal models. In this paper the internal models are modelled

explicitly; in some models of sensorimotor integration these internal models are modelled implicitly. For example, by assuming that the joint angles are known it is implicitly assumed that there exist inverse models of muscle attachments around a joint and of the muscle spindle dynamics (e.g. Mergner and Rosemeier 1998). In the present model, the estimated or internal states can be equated to the perception of external forces acting on the body, support-base displacements and rotations, motion of the visual scene, and orientation of the body in space. Perception of these states can be accessed by psychophysical experiments, by recording of eye movements, or by neural recordings. Predictions of an optimal estimator model for human spatial orientation of angular velocity and tilt perception correspond well to animal neural recordings and human psychophysical data (Borah et al. 1998).

An intriguing question is how an internal representation is obtained. Theoretically it is possible to derive an internal representation from motor outflow and sensory output signals (e.g. Mehra 1971) and also to estimate the precision of different sensory systems from these signals (e.g. Myers and Taply 1976). Although a simple inverted pendulum model was used for body dynamics, there are no fundamental limitations to the inclusion of more segments, dimensions, or muscle models.

Further experiments are necessary to validate the model for a wide variety of experimental settings. Special attention should be drawn to the design of the experiment, since model predictions suggest that postural responses are history dependent. In the future, the adaptive sensory integration model will also be used to model the perception of ego-motion and object motion, when attempting to reproduce well-documented experimental results (Mergner et al. 1991, 1992). The model will be used in combination with experiments to identify and quantify different balance disorders and their causes.

Appendix A: Tapped delay line as predictor for time delays

An optimal estimator for a linear system including time delays is the cascade combination of a Kalman Filter and a predictor (Kleinman 1969). A discrete optimal predictor is a tapped delay line (Fig. A1). The tapped delay line used in this paper is a forward simulation of the discretised dynamics ($A^* = A^{\text{pend}}, B^* = B^{\text{pend}}$) of the pendulum, using known previous control input (u_k) from the delayed estimate made by the adaptive Kalman Filter at t_{k-N}, to the current time t_k. $N = 10$, is determined by the modelled neural time delay ($\tau = 100$ ms) and sample time of the discreet model (unit delay = 10 ms).

Appendix B: Sensor dynamics

The sensory dynamics are approximated by linear transfer functions (Borah et al. 1988).

$$\text{Muscle spindle model: } \frac{\text{afferent fire rate}}{\text{joint angle}} = \frac{5(s+4)}{s+20}$$

$$\text{Semicircular model: } \frac{\text{afferent fire rate}}{\text{angular acceleration}} = \frac{0.574s(s+100)}{(s+0.1)(s+0.033)}$$

$$\text{Otolith model: } \frac{\text{afferent fire rate}}{\text{specific force}} = \frac{90(s+0.1)}{s+0.2}$$

$$\text{Vision model: } \frac{\text{afferent fire rate}}{\text{distance head–visual scence}} = 1$$

$$\text{Tactile model: } \frac{\text{afferent fire rate}}{\text{force}} = \frac{s+0.01}{s+0.1}$$

Appendix C

$$\begin{bmatrix} \theta_k^{\text{sb}} \\ F_k^{\text{ext}} \\ s_k^{\text{sb}} \\ \dot{s}_k^{\text{sb}} \\ \ddot{s}_k^{\text{sb}} \\ s_k^{\text{vis}} \end{bmatrix} = \begin{bmatrix} 1 & 0 & 0 & 0 & 0 & 0 \\ 0 & 1 & 0 & 0 & 0 & 0 \\ 0 & 0 & 1 & T_s & \frac{1}{2}T_s^2 & 0 \\ 0 & 0 & 0 & 1 & T_s & 0 \\ 0 & 0 & 0 & 0 & 1 & 0 \\ 0 & 0 & 0 & 0 & 0 & 1 \end{bmatrix} \begin{bmatrix} \theta_{k-1}^{\text{sb}} \\ F_{k-1}^{\text{ext}} \\ s_{k-1}^{\text{sb}} \\ \dot{s}_{k-1}^{\text{sb}} \\ \ddot{s}_{k-1}^{\text{sb}} \\ s_{k-1}^{\text{vis}} \end{bmatrix} + \begin{bmatrix} 1 & 0 & 0 & 0 \\ 0 & 1 & 0 & 0 \\ 0 & 0 & 0 & 0 \\ 0 & 0 & 0 & 0 \\ 0 & 0 & 1 & 0 \\ 0 & 0 & 0 & 1 \end{bmatrix} \begin{bmatrix} w_{k-1}^{\theta^{\text{sb}}} \\ w_{k-1}^{F^{\text{ext}}} \\ w_{k-1}^{\text{sb}} \\ w_{k-1}^{\text{vis}} \end{bmatrix}$$

$$\Leftrightarrow \underline{x}_k^{\text{env}} = A^{\text{env}} \underline{x}_{k-1}^{\text{env}} + G \underline{w}_{k-1}^{\text{env}} \tag{A1}$$

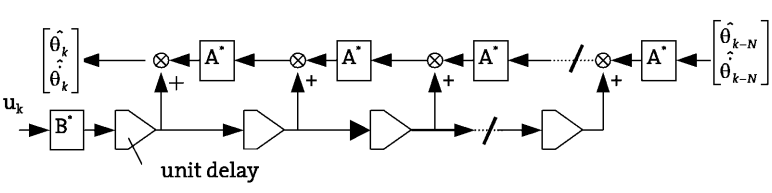

Fig. A1. A tapped delay line to make an optimal prediction of the current spatial orientation from the delayed estimate of spatial orientation as obtained by the adaptive Kalman Filter at t_{k-N}, to the current time t_k. It is a forward simulation of discretised dynamics ($A^* = A^{\text{pend}}$, $B^* = B^{\text{pend}}$) of the pendulum, using known previous control input (u_k), N is number of forward simulation steps and the unit delay is sample time of the discreet model

where T_s is the sample time

$$\begin{bmatrix} w_{k-1}^{\theta^{sb}} \\ w_{k-1}^{F^{ext}} \\ w_{k-1}^{sb} \\ w_{k-1}^{vis} \end{bmatrix} = \begin{bmatrix} \theta_k^{sb} \\ F_k^{ext} \\ \ddot{s}_k^{sb} \\ w_k^{vis} \end{bmatrix} - \begin{bmatrix} \theta_{k-1}^{sb} \\ F_{k-1}^{ext} \\ \ddot{s}_{k-1}^{sb} \\ w_{k-1}^{vis} \end{bmatrix} \Rightarrow \frac{1}{T_s} \begin{bmatrix} w_{k-1}^{\theta^{sb}} \\ w_{k-1}^{F^{ext}} \\ w_{k-1}^{sb} \\ w_{k-1}^{vis} \end{bmatrix}$$

$$\approx \begin{bmatrix} \dot{\theta}_k^{sb} \\ \dot{F}_k^{ext} \\ \dddot{s}_k^{sb} \\ \dot{s}_k^{vis} \end{bmatrix} \tag{A2}$$

Combining (A1) and (A2),

$$E\left\{ \underline{w}^{env} (\underline{w}^{env})^T \right\} \approx T_s^2 E\left\{ \left[\dot{\theta}^{sb} \dot{F}^{ext} \ \dddot{s}^{sb} \dot{s}^{vis} \right]^T \left[\dot{\theta}^{sb} \dot{F}^{ext} \ \dddot{s}^{sb} \dot{s}^{vis} \right] \right\} \tag{A3}$$

Appendix D

For the sake of convenience, the derivation of the estimator for Q is cited literally (Myers and Taply 1976). Consider the linear dynamic state relation at a given time t_j, given by $\underline{x}_j = A\underline{x}_{j-1} + B\underline{u}_{j-1} + \underline{w}_{j-1}$, where $\underline{x}_j$ is an n-vector and $\underline{w}_{j-1} \sim N(q,\ Q)$. The true states $\underline{x}_j$ and $\underline{x}_{j-1}$ are unknown so $\underline{w}_{j-1}$ cannot be determined, but an intuitive approximation $\underline{w}_{j-1}$ is

$$\underline{q}_j \equiv \hat{\underline{x}}_j - A\hat{\underline{x}}_{j-1} - B\underline{u}_{k-1} \tag{A4}$$

where $\underline{q}_j$ is defined as the state noise sample at time t_j. Note that the subscripts j contrast the noise sample from the true unknown mean $\underline{q}$. By hypothesis, the $\underline{w}_{j-1}$ for $j = 1 \rightarrow N$ are independent, and the parameters q and Q are constant. If the $\underline{q}_j$ is assumed to be representative of the $\underline{w}_{j-1}$, they may be considered as independent and identically distributed. Defining a parameter estimation problem, let $\mathscr{R}$ be a random variable on the sample space Ω_2 from which is obtained the data $\underline{q}_j$, $j = 1 \rightarrow N$. Based on the measurements, the unknown distribution of $\mathscr{R}$ characterised by q and C_q is to be estimated.

An unbiased estimator for $\underline{q}$ is the sample mean

$$\hat{\underline{q}} = \frac{1}{N} \sum_{j=1}^{N} \underline{q}_j \tag{A5}$$

An unbiased estimator for Q is obtained by constructing the estimator for C_q, the covariance of $\mathscr{R}$:

$$\hat{C}_q = \frac{1}{N-1} \sum_{j=1}^{N} (\underline{q}_j - \hat{\underline{q}})(\underline{q}_j - \hat{\underline{q}})^T \tag{A6}$$

The expected value of this quantity is

$$E[\hat{C}_q] = \frac{1}{N} \sum_{j=1}^{N} A\hat{P}_{j-1}A^T - \hat{P}_j + Q \tag{A7}$$

An unbiased estimate of Q, after substitution of (A6) is given by

$$\hat{Q} = \frac{1}{N-1} \sum_{j=1}^{N} \left\{ (\underline{q}_j - \hat{\underline{q}})(\underline{q}_j - \hat{\underline{q}})^T - \left(\frac{N-1}{N} \right) \left[A\hat{P}_{j-1}A^T - \hat{P}_j \right] \right\} \tag{A8}$$

Acknowledgements. We would like to thank our colleagues of the Neurologische KlinikNeurozenturm, Freiburg: Prof. Thomas Mergner and his co-workers for stimulating discussions, suggestions and for their warm hospitality during our visits and experimentation in their laboratory.

References

Angelaki DE, McHenry MQ, Dickman JD, Newlands SD, Hess BJ (1999) Computation of inertial motion: neural strategies to resolve ambiguous otolith information. J Neurosci 19: 316–327

Berthoz A, Lacour M, Soechting JF, Vidal PP (1979) The role of vision in the control of posture during linear motion. Prog Brain Res 50: 197–209

Black FO, Shupert CL, Horak FB, Nashner LM (1988) Abnormal postural control associated with peripheral vestibular disorders. Prog Brain Res 76: 263–275

Bolha B, Hlavacka F, Maurer C, Mergner T (1999) Sensory interaction in postural responses to sinusoidal platform rotation. Gait Posture 9[Suppl] 1: S38

Borah J, Young LR, Curry RE (1988) Optimal estimator model for human spatial orientation. Ann NY Acad Sci 545: 51–73

Buchanan JJ, Horak FB (1998 6–7 November) Control of head and trunk position in space in a postural coordination task: the role of the vestibular and visual systems. Proceedings Identifying Control Mechanisms for Postural Behaviours. A satellite meeting to the Society for Neuroscience meeting, Los Angeles

Clark B, Stewart JK (1969) Effects of angular accelerations on man: threshold for perception of rotations and the oculogaryl illusion. Aerosp Med 40: 952–956

Cohen MM, Crosbie RJ, Blackburn LH (1973) Disorienting effects of aircraft catapult launchings. Aerosp Med 44: 37–39

Gelb A (1974) Applied optimal estimation. MIT Press, Cambridge, Mass.

Gerdes VG, Happee R (1994) The use of an internal representation in fast goal-directed movements: a modelling approach. Biol Cybern 70: 513–524

Horak FB, Nashner LM, Diener HC (1990) Postural strategies associated with somatosensory and vestibular loss. Exp Brain Res 82: 167–177

Hosman RJAW (1996) Pilot's perception and control of aircraft. PhD thesis. Delft University of Technology, Delft

Imamizu H, Miyauchi S, Tamada T, Sasaki Y, Takino R, Putz B, Yoshioka T, Kawato M (2000) Human cerebellar activity reflecting an acquired internal model of a new tool. Nature 403: 192–195

Ishida A, Imai S, Fukuoka Y (1997) Analysis of the posture control system under fixed and sway-referenced support conditions. IEEE Trans Biomed Eng 44: 333–336

Jacobs R, van der Kooij H, Burleigh-Jacobs A (1997 22 June) Modelling a new definition of the goal of postural control. Proceedings Multisensory Control of Posture and Gait, 13th International Symposium, Paris

Juang JN, Chen CW, Phan M (1993) Estimation of Kalman filter gain from output residuals. J Guid Control Dynam 16: 903–908

Kawato M, Wolpert D (1998) Internal models for motor control. Novartis Found Symp 218: 291–304

Kleinman DL (1969) Optimal control of linear systems with time-delay and observation noise. IEEE Trans Autom Control 15: 524–527

Maurer C, Mergner T (1999) Postural reaction to platform tilt in normal and subjects and patients with vestibular loss. Gait Posture 9[suppl] 1: S35

Mehra RK (1971) On-line identification of linear dynamic systems with applications to Kalman filtering. IEEE Trans Autom Control 16: 12–21

Merfeld DM, Zupan L, Peterka RJ (1999) Humans use internal models to estimate gravity and linear acceleration. Nature 398: 615–618

Mergner T, Siebold C, Schweigart G, Becker W (1991) Human perception of horizontal head and trunk rotation in space during vestibular and neck stimulation. Exp Brain Res 85: 389–404

Mergner T, Rottler G, Kimmig H, Becker W (1992) Role of vestibular and neck inputs for the perception of object motion in space. Exp Brain Res 89: 655–668

Mergner T, Schweigart G, Kolev O, Hlavacka F, Becker W (1995) Visual-vestibular interaction for human ego-motion perception. In: Mergner T, Hlavacka F (eds) Multisensory control of posture. Plenum, New York, pp 157–168

Mergner T, Rosemeier T (1998) Interaction of vestibular, somatosensory and visual signals for postural control and motion perception under terrestrial and microgravity conditions – a conceptual model. Brain Res Rev 28: 118–135

Mergner T, Glasauer S (1999) A simple model of vestibular canal – otolith signal fusion. Ann NY Acad Sci 871: 430–434

Myers KA, Taply BD (1976) Adaptive sequential estimation with unknown noise statistics. IEEE Trans Autom Control 22: 520–523

Nashner LM, Shupert CL, Horak FB, Black FO (1989) Organisation of posture control: an analysis of sensory and mechanical constraints. Prog Brain Res 80: 411–418

Peterka RJ, Benolken MS (1995) Role of somatosensory and vestibular cues in attenuating visually induced human postural sway. Exp Brain Res 105: 101–110

Runge CF, Shupert CL, Horak FB, Zajac FE (1998) Role of vestibulair information in initiation of rapid postural responses. Exp Brain Res 122: 403–412

Van der Kooij H, Jacobs R, Koopman B, Grootenboer H (1999a) A multisensory integration model of human stance control. Biol Cybern 80: 299–308

Van der Kooij H, Koopman B, Jacobs R, Mergner T, Grootenboer H (1999b 19–21 April) Interpretation of multivariate swaydescriptors. Proceedings Biomechatronics Workshop, University of Twente, Enschede

Wolpert DM, Ghahramani Z, Jordan MI (1995) An internal model for sensorimotor integration. Science 269: 1880–1882

Wolpert DM, Goodbody SJ, Husain M (1998) Maintaining internal representations: the role of the human superior parietal lobe. Nature Neurosci 1: 529–533